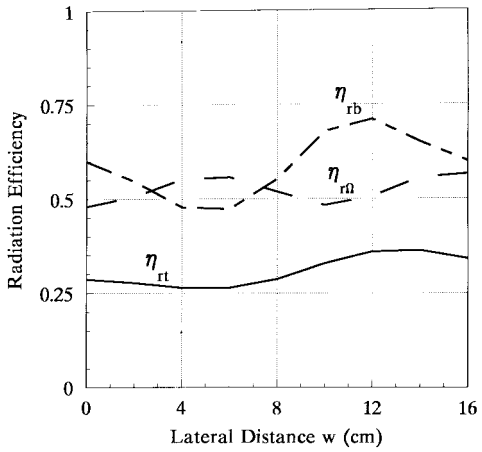

Fig. 5. Computed radiation efficiency of a y-oriented loop antenna proximate to a human body versus the lateral distance w from the center of the human abdomen. Loop radius $b = 1.7$ cm ($kb = 0.1$ at 280 MHz). Wire radius $a = 0.072$ cm (Hallen factor $2\ln(2\pi b/a) = 10$).

range. It is also noted that compared with the loop in free space, the noise temperature is approximately 30 K lower for the y-oriented loop proximate to the body when frequency is higher than 280 MHz. Table I also shows the maximum/minimum directive and power gains of the y-oriented loop in the H-plane at 280 MHz. For the E_θ pattern, although maximum directive gain is reduced from 1.52 dB in free space to -3.9 dB due to the body blocking and absorption effects, the maximum power gain is enhanced from -5.93 to -1.49 dB. This is contributed by the enhancement of the ohmic-loss efficiency by the body. The highly increasing of the minimum directive gain (from -100 dB to -9 dB) and power gain (from -100 dB to -14.47 dB) when proximate to the body also indicates the positive effect of the human body.

IV. Conclusion

Analysis and numerical computation of EM coupling between a circular loop antenna with different orientations and a full-scale human-body model from 50 to 400 MHz have been performed. The body has the highest absorption rate of the radiated power from the x-oriented loop antenna. Hence, the x-oriented loop may be suitable for the hyperthermia-applicator application to achieve efficient power deposition. The y- and z-oriented loop antennas are suitable for personal wireless-communication applications by considering the radiation efficiency and power patterns. Numerical results for the antenna input impedance, radiation patterns/polarization level, radiation efficiency, and power gain are important for the applications of different aspects.

References

[1] J. Toftgard, S. N. Hornsleth, and J. B. Andersen, "Effects on portable antennas of the presence of a person," *IEEE Trans. Antennas Propagat.*, vol. 41, pp. 739–746, June 1993.

[2] H.-R. Chuang, "Human operator coupling effects on radiation characteristics of a portable communication dipole antenna," *IEEE Antennas Propagat.*, vol. 20, pp. 556–560, Apr. 1994.

[3] M. A. Jensen and Y. Rahmat-Samii, "EM Interaction of handset antennas and a human in personal communications," *Proc. IEEE*, vol. 83, pp. 1–17, Jan. 1995.

[4] K. Fujimoto and J. R. James, *Mobile Antenna Systems Handbook*. Norwood, MA: Artech House, 1996, ch. 4.

[5] K. Ito, I. Ida, and M. Wu, "Body effect on characteristics of small loop antenna in pager systems" in *IEEE AP-S Int. Symp. Dig.*, vol. 2, Chicago, IL, July 1992, pp. 1081–1084.

[6] J. S. Colburn and Y. Rahmat-Samii, "Electromagnetic scattering and radiation involving dielectric objects," *J. Electromag. Waves Applicat.*, vol. 9, no. 10, pp. 1249–1277, 1995.

[7] H.-R. Chuang and W.-T. Chen, "Numerical modeling of EM coupling between a loop antenna and a 3-D lossy body object," in *Int. Symp. EMC*, Rome, Italy, Sept. 1996, pp. 204–209.

[8] J. Van Bladel, "Some remarks on Green's dyadic for infinite space," *IRE Trans. Antennas Propagat.*, vol. AP-9, pp. 563–566, 1961.

[9] D. E. Livesay and K. M. Chen, "Electromagnetic fields induced inside arbitrarily shaped biological bodies," *IEEE Trans. Microwave Theory Tech.*, vol. MTT-22, pp. 1273–1280, Dec. 1974.

[10] K. M. Chen, "A simple physical picture of tensor Green's function in source region," *Proc. IEEE*, vol. 65, pp. 1202–1204, Aug. 1977.

[11] D. P. Nyquist, K. M. Chen, and B. S. Guru, "Coupling between small thin-wire antennas and a biological body," *IEEE Trans. Antennas Propagat.*, vol. AP-25, pp. 863–866, Nov. 1977.

[12] A. D. Yaghjian, "Electric dyadic Green's functions in the source region," *Proc. IEEE*, vol. 68, pp. 248–263, Feb. 1980.

[13] K. Karimullah, K. M. Chen, and D. P. Nyquist, "Electromagnetic coupling between a thin-wire antenna and a neighboring biological body: Theory and experiment," *IEEE Trans. Microwave Theory Tech.*, vol. 28, pp. 1218–1225, Nov. 1980.

[14] J. D. Kraus, *Antennas*. New York: McGraw-Hill, 1988, ch. 6.

[15] C. C. Johnson and A. W. Guy, "Nonionizing electromagnetic wave effects in biological materials and systems," *Proc. IEEE*, vol. 60, pp. 692–718, June 1972.

New Tunable Phase Shifters Using Perturbed Dielectric Image Lines

Ming-yi Li and Kai Chang

***Abstract*—This paper presents new tunable phase shifters using perturbed dielectric image lines (DIL's). The propagation constant in the DIL was perturbed by a movable metal reflector plate installed in parallel with the ground plane of the DIL. The phase shift was thus controlled and adjusted by varying the perturbation spacing between the DIL and movable reflector plate at a given operating frequency. A rigorous hybrid-mode analysis was used for calculating the dispersion of propagation constants in the perturbed DIL, and then for designing tunable phase shifters. *Ka*-band tunable phase shifters have been designed, fabricated, and tested. Measurement results agree well with theoretical predictions. The device is especially useful for millimeter-wave applications where traditional phase shifters are lossy.**

***Index Terms*—Dielectric image lines, millimeter waves, tunable phase shifters.**

I. Introduction

Dielectric image lines (DIL's) have reduced losses compared to microstrip lines at millimeter-wave frequencies since most of the signal travels in the low-loss dielectric region [1]. This structure

Manuscript received July 17, 1997; revised May 5, 1998. This paper originally appeared in the September 1998 issue of this TRANSACTIONS and is being reprinted here with the correct graphics. This work was supported by the NASA Lewis Research Center and the Texas Higher Education Coordinating Board's Advanced Technology Program.

The authors are with the Department of Electrical Engineering, Texas A&M University, College Station, TX 77843-3128 USA.

Publisher Item Identifier S 0018-9480(98)06150-X.

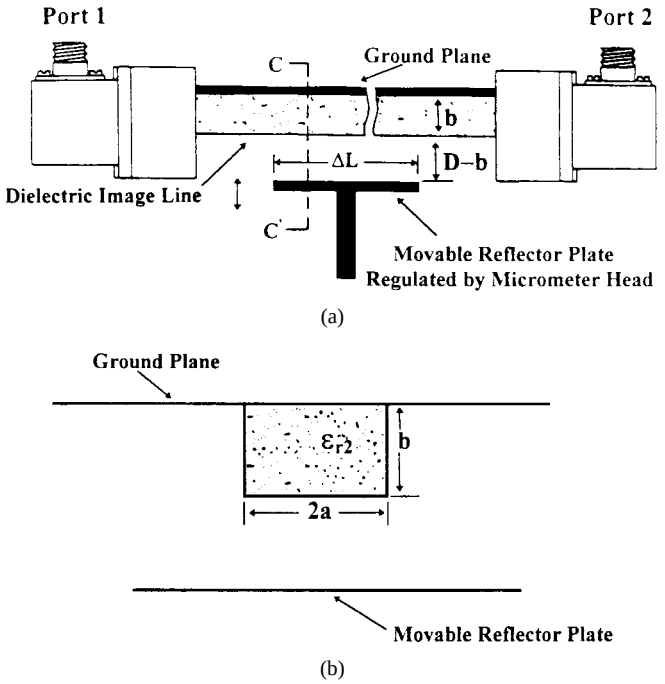

Fig. 1. (a) Structure of a tunable phase shifter using a perturbed DIL. (b) Cross-sectional view at $C - C'$.

was recently proposed for feeding the aperture-coupled microstrip-patch antenna arrays [2]–[4], and overcomes the high conduction loss problem of microstrip lines at millimeter-wave frequencies. A phase shifter is one of the important control circuits used extensively at microwave and millimeter-wave frequencies. Traditional phase shifters use solid-state or ferrite devices. In this paper, new tunable phase shifters using DIL's are described. The DIL can be transformed to rectangular waveguide or microstrip line using transitions.

In a DIL, the electromagnetic (EM) signal travels mainly inside the dielectric and can be perturbed in several ways. The changing of propagation constants of an EM field in the DIL can be applied to vary the phase difference. This paper reports the perturbation of propagation constant in the DIL by a movable metal reflector plate installed in parallel with the ground plane of the DIL. The phase shift was controlled and adjusted by changing the perturbation spacing between the DIL and movable reflector plate at an operating frequency. The movement can be controlled mechanically or electromechanically using a motor or piezoelectric materials. The tunable range of phase shifters principally relies on the dispersion property of EM-wave propagation constants in DIL's. The structure is simple, low-cost, easy to be fabricated, stable, and reliable.

The DIL was generally analyzed using the effective dielectric constant (EDC) method [1], [5], [6]. It is an approximate calculation and cannot be used to analyze the perturbed DIL structure with a movable reflector plate (DILWRP). In this paper, a rigorous hybrid-mode analysis was used for calculating the dispersion of EM-field propagation constants in the perturbed DIL structures, and then for designing tunable phase shifters. *Ka*-band tunable phase shifters using a DILWRP have been designed, fabricated, and tested. It had good impedance match, wide frequency operation, and large tunable ranges. Experimental results agree very well with theoretical predictions.

II. Configurations

Fig. 1(a) shows the structure of a tunable phase shifter using a perturbed DIL, and Fig. 1(b) shows the cross-sectional view at $C - C'$. A movable metal reflector plate is installed in parallel with the ground plane of the DIL to form a DILWRP structure. The perturbation spacing between the DIL and movable reflector plate is controlled and precisely adjusted using a micrometer head. For testing purposes, the signal is coupled to the DIL from the waveguide through transitions. Proper design of DIL dimensions allows single-mode propagation for a considerable range of frequency [1]. The phase shift between ports 2 and 1 of the structure without a movable reflector plate depends on the length of the DIL and the propagation constant in the DIL

$$\Phi_{21} = L \cdot \beta_g + \Phi_0 \tag{1}$$

where L is the length of the DIL, $\beta_g = 2\pi/\lambda_g$ is the propagation constant in the DIL, and Φ_0 is the phase due to transitions and connections, which can be calibrated out using proper calibration techniques. The propagation constant β_g in the DIL is changed when a movable metal reflector plate is installed and the perturbation spacing is varied. This results in a tunable phase shift

$$\Delta\Phi_{21} = \Delta L \cdot \Delta\beta_g \tag{2}$$

where ΔL is the perturbation length in the DIL, and $\Delta\beta_g$ is the perturbed propagation constant in DIL. The tunable range of the phase shifter is controlled by ΔL and $\Delta\beta_g$, and may be raised by making ΔL larger and increasing the perturbation of propagation constants $\Delta\beta_g$. The structure of tunable phase shifters given above is simple, low-cost, easy to fabricate, and reliable. The phase shifts can be easily controlled.

III. Rigorous Hybrid-Mode Analysis and Theoretical Results

Accurate computation of propagation constants and λ_g in the perturbed DIL with a movable reflector plate is required for theoretically predicting the phase shifts. A rigorous hybrid-mode analysis [7] was used in this paper for calculating the dispersion of propagation constants in the DILWRP and then for designing tunable phase shifters.

Fig. 2 is the configuration of a DIL of width $2a$, height b, and relative dielectric constant ε_{r2}. A movable perfect electric reflector plate is placed at a distance D $(z = -D)$ in parallel with the ground plane $(z = 0)$. The perturbation of the reflector plate to EM field properties in the DILWRP can be adjusted by changing the distance D. DILWRP structures will become DIL when D increases to infinity. The cross-section region with DIL under the ground plane is subdivided into four subregions I–IV. A complete set of field solutions is derived for each subarea. The dependence of field components on x can be assumed to be an exponential function as $\exp(\pm j\beta_g x)$. β_g is the phase propagation constant and is the same in all these four subregions. y- and z-dependencies of fields in regions I–IV are formulated using eigenfunctions, so that boundary conditions are fulfilled on defined boundaries. All modes are classified as TM and TE with respect to the z-direction. Fields in every subregion can be expressed in terms of scalar potential functions for TM and TE to z-modes. Boundary conditions are enforced independently. Finally, a complex matrix equation is derived. All matrix elements are functions of frequency f, perturbation spacing D, image line sizes, dielectric constant ε_{r2}, and propagation constant β_g. All data except β_g in these matrix elements can be calculated when f, D, image line sizes, and ε_{r2} are given. Propagation constants β_g in the DILWRP are computed by determining the zeros of the determinant of the whole complex matrix equation. The effect of different perturbation spacing D on propagation constants β_g is then accurately computed.

For a given operating frequency and DILWRP structure characteristics, the determinant of the complex matrix is computed and examined

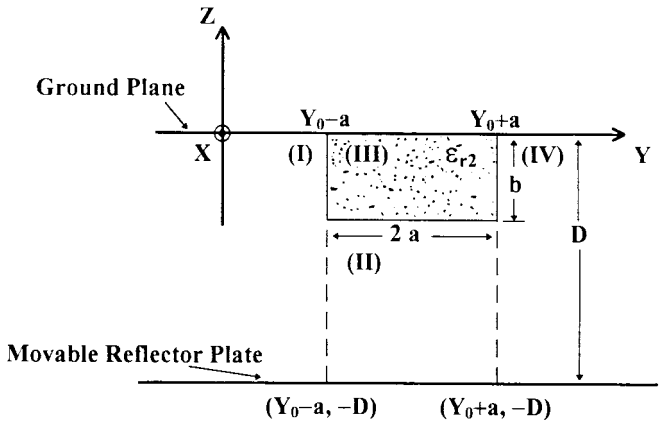

Fig. 2. DILWRP.

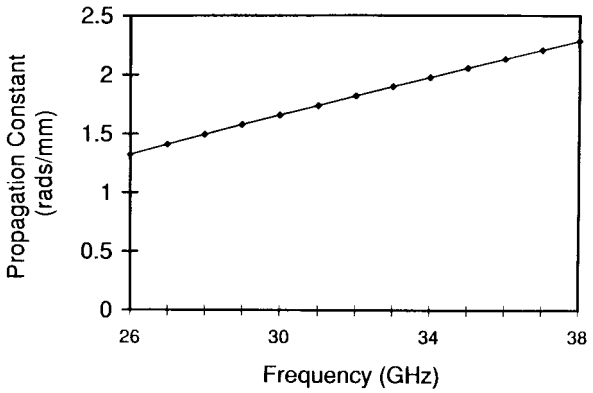

Fig. 3. Calculated propagation constants β_g for the *Ka*-band DILWRP. Image line sizes: 1.27 mm × 2.54 mm, $\varepsilon_{r2} = 10.5$, $D = 10.0$ mm.

for its zero crossing for β_g in the range between β_0 and $\beta_0\sqrt{\varepsilon_{r2}}$. Propagation constants β_g are then determined. The complex double precision is used in calculating the determinant. A sufficient number of imaginary roots has to be solved and used, and the right imaginary roots have to be chosen in order to get convergent and accurate numerical results. The correct way to choose real and imaginary roots has been studied and found in this paper. Accurate results and fast convergence can be achieved using only five TE modes and five TM modes, which include four real modes and one imaginary mode.

Fig. 3 shows calculated results β_g for *Ka*-band DILWRP structures. The relative dielectric constant of the DIL in all cases was 10.5. Image line sizes were 1.27 mm × 2.54 mm. The perturbation distance D was chosen as 10.0 mm. Five TE modes and five TM modes were used in all computation with a calculation accuracy better than 1%. Results of propagation constants β_g were found to increase when the operating frequency increased. Propagation constants β_g in the DILWRP have been seen to be different when the perturbation distance D changes. Fig. 4 gives numerical results of β_g in the *Ka*-band DILWRP for different distance D at 29.0 and 35.0 GHz. β_g was found to increase 11.5% at 29.0 GHz and 5.71% at 35.0 GHz when distance D decreased from 10.0 to 1.3 mm. The EDC method is an approximate method and can be used only for an image line without reflector plate, which is the special case of the DILWRP with an infinitive perturbation spacing D. The H-guide is another special case of the DILWRP when D is equal to the thickness b of the DIL. Calculated results using the EDC method [1], [5], [6] and H-guide theory [1] are also given in Fig. 4 for comparison. It can be seen that

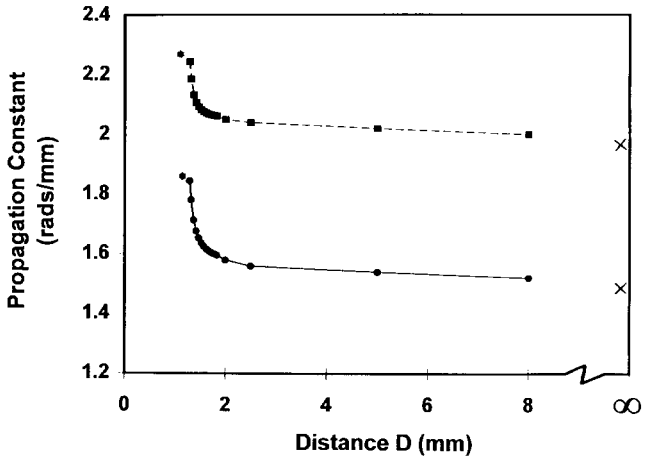

Fig. 4. Computed propagation constants β_g for the *Ka*-band DILWRP with different distance D at 29.0 and 35.0 GHz. Image line sizes: 1.27 mm × 2.54 mm, $\varepsilon_{r2} = 10.5$. —●—: 29.0 GHz, –■–: 35.0 GHz, hybrid mode analysis: × EDC method, ∗: H-guide theory.

theory agrees well with the results calculated using the EDC method and H-guide theory for these two special cases.

IV. Experimental Results

Operating frequency range, propagation constants β_g in the DIL, perturbation spacing D, and the effect of different D on β_g are several key parameters for designing tunable phase shifters using the DILWRP. They determine the tunable range of a phase shifter. Ideally, the DIL should be kept as large as possible at a given operating frequency range, especially for millimeter-wave applications, in order to ease fabrication problems and lessen the effects of size variations on the guide wavelength and scan angle. At the same time, single-mode operation must be maintained in the propagation of the signal in the DIL in order to achieve accurate phase shifts. The unit ratio of the DIL size of $a/b = 1$ provides the maximum bandwidth [1]. For good field containment and single-mode operation, the following formula can be used to select unit aspect ratio a/λ_0 for DIL structures:

$$\frac{a}{\lambda_0} \approx \frac{0.32}{\sqrt{\varepsilon_{r2} - 1}}. \tag{3}$$

The relative dielectric constant ε_{r2} of the DIL should be chosen not too small in order to get enough dispersion in DIL's, and then to realize large phase-shift ranges. $\varepsilon_{r2} = 10.5$ is a good choice for the *Ka*-band frequency range from our experience.

The rigorous hybrid mode analysis was used to design the DILWRP. RT-Duroid material of relative dielectric constant $\varepsilon_{r2} = 10.5$ was used to make the DIL. The *Ka*-band DIL had $2a = 3.00$ mm and $b = 1.27$ mm. A diameter of 6.0 mm of the movable reflector disk was installed in parallel with the ground plane of the DIL to form a DILWRP. The perturbation length ΔL was then equal to 6.0 mm. A micrometer head was used to precisely control the perturbation distance to an accuracy of 1 mil.

The *Ka*-band tunable phase shifter showed good input impedance match, low insertion loss, wide frequency operation, and large tuning phase-shift range. Fig. 5 gives satisfied measurement results of the insertion loss in an *Ka*-band tunable phase shifter. Less than 2.0-dB insertion loss was realized, which included losses in the DIL with a length of 110 mm and in two waveguide-to-DIL transitions. The movable reflector plate did not deteriorate the performance of insertion loss and return loss even when the perturbation spacing $(D - b)$ was close to 1 mm. Fig. 6 shows experimental and theoretical

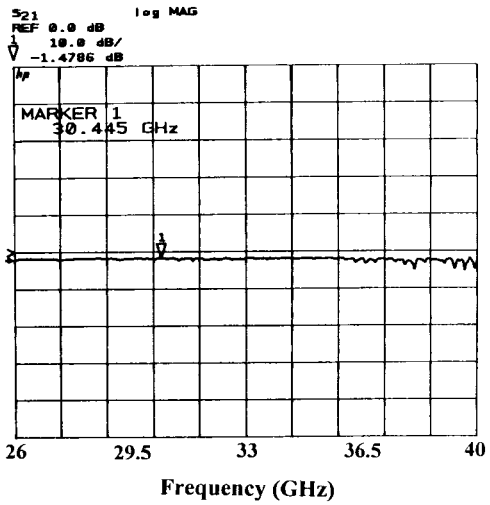

Fig. 5. Experimental insertion loss results of the *Ka*-band tunable phase shifter, which includes all losses in the DIL and in two waveguide-to-DIL transitions.

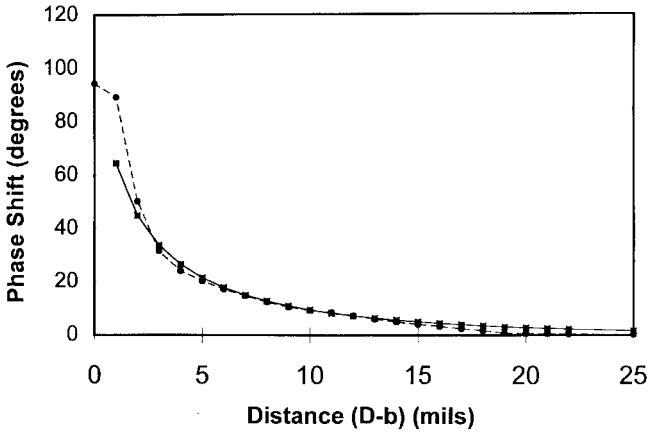

Fig. 6. Phase shifts for different perturbation spacing $(D - b)$ at 35 GHz. –■–: theoretical, –●–: experimental.

results of phase shifts for different perturbation spacing $(D - b)$ at 35 GHz. Tuning ranges approximately 90° were reached for the perturbation length $\Delta L = 6.0$ mm when the perturbation spacing $(D - b)$ changed from 25 to 1 mil. The tuning range of phase shifts can be increased further using longer ΔL. Measurement data agreed well with theory prediction in all operating frequencies.

V. Conclusions

New tunable phase shifters using perturbed DIL's have been presented in this paper. The propagation constant in the DIL was perturbed by a movable metal reflector plate installed in parallel with the ground plane of the DIL. A micrometer head was used to precisely control the perturbation spacing. The phase shift was adjusted by varying the perturbation spacing at a given operating frequency. A rigorous hybrid-mode analysis was used for calculating the dispersion of propagation constants in the DIL, and then for designing tunable phase shifters. The structure is simple, low-cost, easy to fabricate, stable, and reliable.

Ka-band tunable phase shifters using the DILWRP have been designed, fabricated, and tested. Tunable phase shifters showed good impedance match, low insertion loss, wide frequency operation, and large tuning phase-shift range. Less than 2.0-dB insertion loss was realized, which included all losses in the DIL and in two waveguide-to-DIL transitions. The movable reflector plate did not deteriorate the performance of insertion loss and return loss of the phase shifter even when the perturbation spacing $(D - b)$ was close to 1 mm. Tuning ranges approximately 90° were accomplished for the perturbation length $\Delta L = 6.0$ mm, and could be increased further using longer ΔL. Measurement data agreed well with theoretical predictions.

Acknowledgment

The authors would like to thank Dr. S. Kanamaluru and Dr. J. A. Navarro for their helpful suggestions and useful discussion.

References

[1] P. Bhartia and I. J. Bahl, *Millimeter Wave Engineering and Applications*. New York: Wiley, 1984.

[2] M. Y. Li, S. Kanamaluru, and K. Chang, "Aperture coupled beam steering microstrip antenna array fed by dielectric image line," *Electron. Lett.*, vol. 30, pp. 1105–1106, July 1994.

[3] S. Kanamaluru, M. Y. Li, and K. Chang, "Design of aperture coupled microstrip antenna array fed by dielectric image line," *Electron. Lett.*, vol. 31, pp. 843–845, May 1995.

[4] ____, "Analysis and design of aperture coupled microstrip patch antennas and arrays fed by dielectric image line," *IEEE Trans. Antennas Propagat.*, vol. 44, pp. 964–974, July 1996.

[5] R. M. Knox and P. P. Toulious, "Integrated circuits for the millimeter through optical frequency range," in *Proc. Symp. Submillimeter Waves*, New York, NY, Mar. 1970, pp. 497–516.

[6] T. Itoh and B. Adelseck, "Trapped image guide for millimeter wave circuits," *IEEE Trans. Microwave Theory Tech.*, vol. MTT-28, pp. 1433–1436, Dec. 1980.

[7] K. Solbach and I. Wolff, "The electromagnetic fields and the phase constants of dielectric image lines," *IEEE Trans. Microwave Theory Tech.*, vol. MTT-26, pp. 266–274, Apr. 1978.